Strain effects on ensemble populations in AuPd/Pd(100) surface alloys

J. Adam Stephens and Gyeong S. Hwang

Citation: The Journal of Chemical Physics **139**, 164703 (2013); doi: 10.1063/1.4825396
View online: http://dx.doi.org/10.1063/1.4825396
View Table of Contents: http://scitation.aip.org/content/aip/journal/jcp/139/16?ver=pdfcov
Published by the AIP Publishing

Strain effects on ensemble populations in AuPd/Pd(100) surface alloys

J. Adam Stephens and Gyeong S. Hwang[a)]
Department of Chemical Engineering, University of Texas at Austin, Austin, Texas 78712, USA

(Received 10 February 2013; accepted 3 October 2013; published online 23 October 2013)

The effects of applied strain on the arrangement of atoms in AuPd/Pd(100) surface alloys are studied using Monte Carlo simulations and cluster expansion Hamiltonians. The strain effects are found to be significant, with heteronuclear (Au-Pd) interactions more strongly enhanced by biaxial compression than homonuclear (Pd-Pd) ones. In particular, compressive strain causes an increase in the population of Pd monomers and second nearest-neighbor pairs of Pd monomers, both of which have been identified previously as important ensembles for various catalytic reactions. We also discuss the origin of these effects using density functional theory calculations of the surface electronic structure of strained AuPd/Pd(100).Our findings may suggest an additional means of employing strain to tune the catalytic properties of surface alloys. © *2013 AIP Publishing LLC*. [http://dx.doi.org/10.1063/1.4825396]

I. INTRODUCTION

The addition of gold (Au) to palladium (Pd) has been found in many cases to greatly improve its catalytic performance. AuPd alloys have been shown, for instance, to promote the direct synthesis of hydrogen peroxide from hydrogen (H_2) and oxygen (O_2),[1,2] vinyl acetate synthesis,[3–5] and the selective oxidation of alcohols to aldehydes.[6] The enhanced catalytic properties of AuPd often can be attributed to its ability to form stable mixed alloy surfaces in which *ensembles* of Au and Pd atoms act to promote the formation of desirable products and inhibit undesirable side reactions. For example, second nearest-neighbor pairs of Pd monomers were shown by Chen *et al.* to play an important role in vinyl acetate synthesis on the AuPd(100) surface.[3,4] Calculations reported by Hwang and co-workers suggested that Pd monomers in AuPd(111) may prevent O–O bond scission in adsorbed O_2, facilitating H_2O_2 synthesis;[7,8] their calculations also demonstrated that small groups of Pd atoms may be active sites for CO oxidation, preventing poisoning of the surface.[9] Surface Pd monomers also were determined by Wang *et al.* to have a substantial effect on the activity of carbon supported AuPd nanoparticles toward glycerol oxidation.[10]

Because of the importance of the ensemble effect in explaining their improved catalytic performance, numerous studies have been undertaken to ascertain and control the surface atomic configuration of AuPd alloys. Using scanning tunneling microscopy (STM), Maroun *et al.*[11] counted Pd monomers, dimers, and trimers in monolayer AuPd surface alloys on Au(111) substrates. The Goodman group conducted a number of studies on (100) and (111) surface facets of bulk and thin, multilayer AuPd alloys to identify and count surface ensembles using various experimental techniques.[12–14] Boscoboinik *et al.* developed a model based on first neighbor pair interactions in AuPd(111) surface alloys which they have used to examine the distribution of surface Pd atoms as a function of surface concentration[15] and to count specific adsorption sites.[16] Using similar methods, Garvey *et al.* made a study of the AuPd/Pd(100) surface using longer range interactions.[17] And, recently, Stephens and Hwang[18,19] compared the atomic configuration of AuPd surface alloys to AuPt in both the (111) and (100) surface facets. These experimental and computational studies systematically investigated the influence of surface composition, bulk composition, annealing temperature, and other factors on the arrangement of atoms in the surfaces of AuPd alloys. By contrast, one "variable" that we believe has received little explicit attention is strain. Although the influence of strain on the surface reactivity of various metals is relatively well understood,[20–29] as far as we know, no studies of its potential effects on the arrangement of atoms in surface alloys have been reported. Owing to the demonstrated importance of ensemble effects in AuPd, this is a question that we wished to address.

In this article, we examine the influence of strain on the atomic arrangement of AuPd/Pd(100) surface alloys. For each of the strain conditions considered, we first generate a cluster expansion (CE) Hamiltonian from the results of density functional theory (DFT) calculations, which we then use in canonical ensemble Metropolis Monte Carlo (MC) simulations to predict the atomic ordering of larger AuPd/Pd(100) surfaces at finite temperatures. We find that under compressive strain, the tendency of the surface to form Pd monomers and to retain $c(2 \times 2)$-like ordering are increased compared to the strain-free case, while under tensile strain, they are reduced. We also performed an analysis of the surface electronic structure of two ordered AuPd/Pd(100) alloys to further elucidate the origin of these strain effects. The fundamental findings may suggest an additional means of tailoring and improving the catalytic properties of AuPd alloys.

II. METHODOLOGY

A. Cluster expansion method

In the cluster expansion formalism, every site in a lattice is first assigned an occupation variable. The value of the variable is determined by the alloy constituent that occupies

a)Author to whom correspondence should be addressed. Electronic mail: gshwang@che.utexas.edu

the site. The energy of the lattice is then expanded in terms of products of spatial clusters of the site variables. It can be shown that these products form a complete basis, which can in principle exactly represent the energy;[30] however, in practice, a CE must be truncated. Even so, cluster expansions that have been parameterized using appropriately constructed training sets of DFT calculated energies are commonly capable of energy predictions within a few meV/atom of DFT.[31–37]

In this work, we chose to model the energetics of the strained AuPd/Pd(100) surface by preparing separate CEs for each of the strain conditions that we considered, each having its own training set of model surfaces (described in the following section). Cross validation score minimization[38] was used to select from among candidate 2-body clusters with up to 5th nearest-neighbor interactions and 3- and 4-body clusters with up to 4th nearest-neighbor interactions. To improve sampling of the low energy region of the potential energy surface, the training sets were also iteratively expanded to include global minima as they were discovered by candidate CEs. The procedure we followed is described in greater detail in Refs. 18 and 19.

The final CE for the compressive strain case contained a total of 14 clusters, and the associated training set contained 51 model surfaces. For the strain-free and tensile cases, these quantities were (14 clusters, 45 surfaces) and (15 clusters, 49 surfaces), respectively. The expansions along with some additional details pertaining to their creation are included in the supplementary material.[39]

B. Density functional theory

Spin-polarized DFT calculations within the generalized gradient approximation (GGA-PW91[40]) were performed using the Vienna *Ab-initio* Simulation Package (VASP).[41] The projector augmented wave (PAW) method with a planewave basis set was employed to describe the interaction between core and valence electrons.[42] The valence configurations employed to construct the ionic pseudopotentials are $5d^{10}\ 6s^1$ for Au and $4d^9\ 5s^1$ for Pd. An energy cutoff of 350 eV was applied for the planewave expansion of the electronic eigenfunctions. For Brillouin zone integration in the model surfaces, a $(6 \times 6 \times 1)$ Monkhorst-Pack mesh of k-points was used.

The models used to represent AuPd/Pd(100) surfaces in our DFT calculations were four layer slabs, each consisting of a 4×4 AuPd(100) surface layer atop three additional (100) layers of pure Pd. The top and bottom of the slabs were separated through a periodic boundary by the equivalent of 7 atomic layers. The bottom two layers were fixed at bulk positions, and the top two were relaxed until all the atomic force components were smaller than 0.03 eV/Å. Biaxial strain was simulated by uniformly changing the surface-parallel dimensions of the supercell by −2%, 0%, or +4% of the bulk Pd value, which was determined by DFT to be 3.961 Å. The surface-perpendicular separation of the fixed Pd layers was also adjusted to account for strain-induced relaxation in that direction. The extent of the relaxation was determined by applying biaxial strain to a bulk Pd sample, then minimizing the energy with respect to the supercell size along the perpendicular direction. The ratio of applied strain to response determined from these calculations is −0.689 and −0.586 for 2% compression and 4% tension, respectively, which closely match a Hooke's law-based prediction made using experimentally measured 0 K elastic stiffness constants for Pd(−0.665).[43]

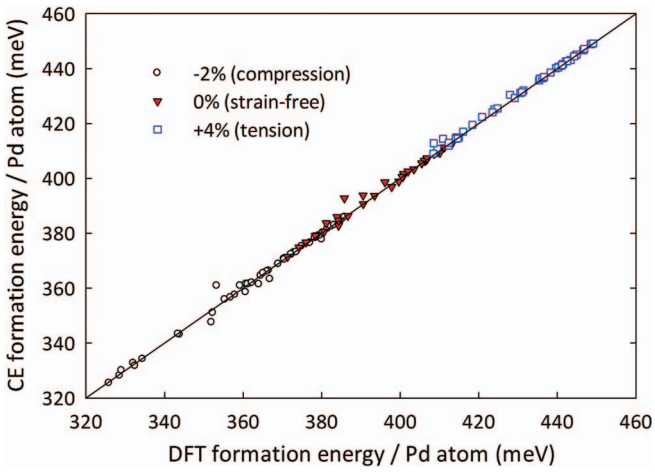

FIG. 1. Formation energies per surface Pd atom (E_f/N_{Pd}) of the model surfaces in each training set, where $E_f = E_{AuPd} - (E_{Au} + N_{Pd} \cdot \Delta E_{Pd-Au})$. In this expression, E_{AuPd} and E_{Au} are, respectively, the total energies of the model surface in question and a model surface with a pure Au surface layer, ΔE_{Pd-Au} is the difference in the cohesive energies of bulk Pd and Au, and N_{Pd} is the number of surface Pd atoms.

Predictions made using the cluster expansions are compared to DFT results in Figure 1. Each point represents the formation energy (on a per Pd atom basis, defined in the caption) of a model surface from the CE training sets. The energies span a range of approximately 140 meV, and the CE predictions exhibit only very small departures from the DFT reference energies.

C. Monte Carlo simulation

Once completed, the three cluster expansions were incorporated into canonical ensemble Monte Carlo simulations of the AuPd/Pd(100) surface. All of the surfaces we simulated contained 30×30 (100) surface unit cells for a total of 900 atoms. The surfaces were first annealed at high temperature and then cooled and equilibrated at the simulation temperature over a period of 7×10^5 steps per site. Properties of the atomic configuration were then calculated and averaged over 1×10^5 steps per site. The candidate configurations evaluated at the beginning of each step were generated by swapping randomly selected Au and Pd atoms. Past experience has shown this procedure to be adequate to erase any bias from the initial configuration and to achieve consistency between repeated runs at the same simulation temperature and composition.

III. RESULTS AND DISCUSSION

Figure 2 shows snapshots from simulations of select AuPd/Pd(100) surfaces with different composition ratios and degrees of strain. While some qualitative trends may be

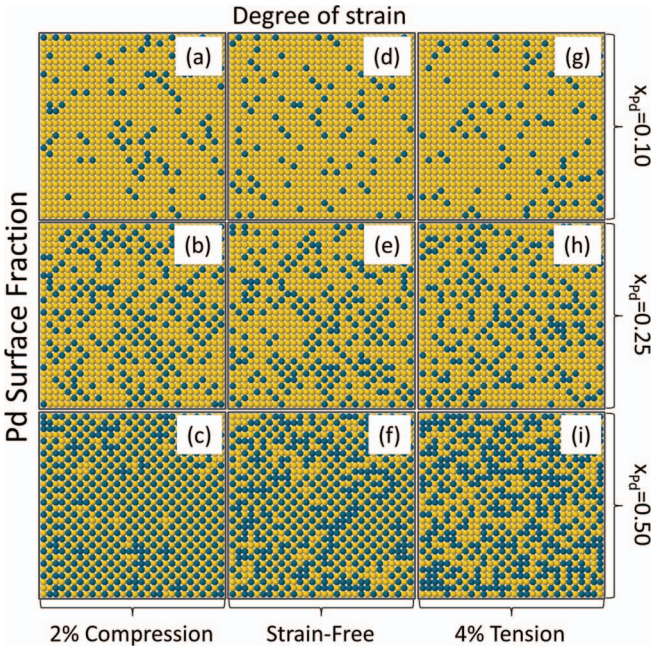

FIG. 2. Snapshots from MC simulations of AuPd/Pd(100) under different strain conditions and with different Pd surface fraction, x_{Pd}.

evident from the images, they are chiefly intended to complement and aid in the interpretation of the results which will be presented in Figures 3 and 4, in which each "point" is an average over all the configurations visited in the course of a separate MC simulation, as just discussed.

Figure 3 shows the effect of strain on the population of Pd monomers in AuPd/Pd(100) at $T = 300$ K. The monomer population is found to be increased by compression and reduced by tension, relative to the strain-free case, over the entire composition range considered. The strain effect becomes greatest at a Pd atomic fraction of $x_{Pd} = 0.45$–0.50, where the population of monomers in the compressively strained surface is about 1.8 and 3.3 times larger than in the strain-free and tensile cases, respectively.

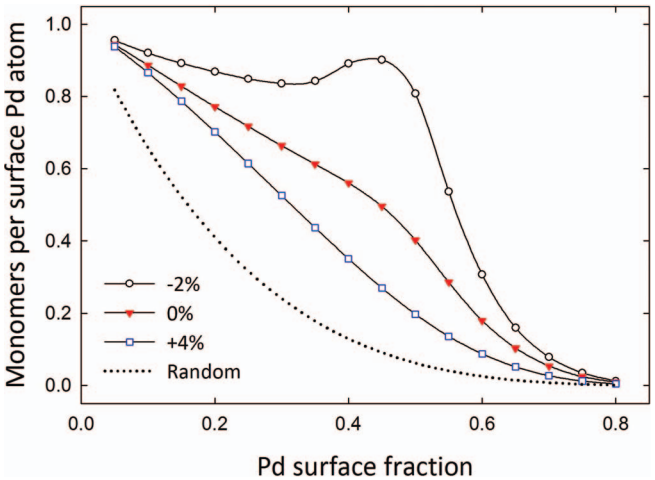

FIG. 3. Number of Pd monomers per surface Pd atom at $T = 300$ K, obtained from MC simulation, under compressive (−2%), strain-free (0%), and tensile (+4%) conditions.

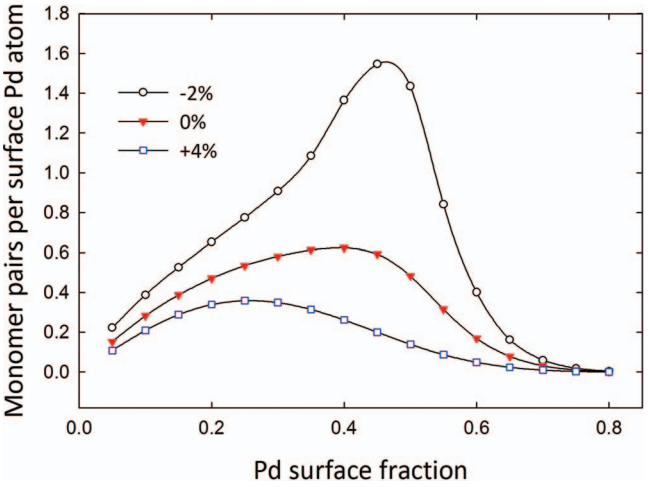

FIG. 4. Number of 2NN pairs of Pd monomers per surface Pd atom at $T = 300$ K, obtained from MC simulation, under compressive (−2%), strain-free (0%), and tensile (+4%) conditions.

It can also be seen that under all three strain conditions (−2%, 0%, and 4%), the population of monomers is larger in the AuPd/Pd(100) surface than in a random alloy (which has no interatomic interactions).Our previous studies (Refs. 18 and 19) showed that Pd monomers form in greater-than-expected numbers because of a preference for heteronuclear (Au-Pd) over homonuclear (Au-Au, Pd-Pd) interactions. The differences between the population of monomers in the strained surfaces suggest that compressive strain strengthens the heteronuclear interactions relative to homonuclear ones, and that tensile strain weakens them.

Due to their importance in a number of surface reactions, we next considered how strain affects the population of 2NN pairs of Pd monomers. In Figure 4, we plot the number of 2NN pairs per surface Pd atom as a function of x_{Pd} and degree of strain, as obtained from MC simulations at $T = 300$ K. The number of 2NN pairs is increased by compressive strain and reduced by tensile strain. The strain effect becomes especially pronounced in the region of $x_{Pd} = 0.5$, where the number of pairs in the compressed surface is almost 8 times greater than in the tensile case.

The origin of this sizeable difference between the compressive and tensile surfaces at $x_{Pd} = 0.5$ can be clarified by examining the last row of snapshots in Figure 2. In particular, the compressed [Fig. 2(c)] surface appears to be well ordered, with several extended $c(2 \times 2)$-like patches. Note that in the (100) surface facet, $c(2 \times 2)$ order maximizes the number of monomers and 2NN monomer pairs. Patches of $c(2 \times 2)$ order also exist in the strain-free surface [Fig. 2(f)], but are visibly smaller, and in the 4% tensile case [Fig. 2(i)], they have nearly vanished.

This effect of strain on ordering can be measured using the Warren-Cowley short range order (SRO) parameter,[44] which we restrict here to the first nearest neighbor shell,

$$\alpha = 1 - \frac{p_{AB}}{x_B}. \quad (1)$$

In Eq. (1), p_{AB} is the probability (in an alloy of A and B atoms) that a first nearest neighbor of a randomly selected

A atom will be a B atom, and x_B is the fraction of B atoms in the surface layer. In a completely random alloy, there is no tendency for A atoms to preferentially attract either A or B atoms into their 1NN shells, so $p_{AB} = x_B$, and therefore $\alpha = 0$. On the other hand, in a AuPd(100) surface alloy with $x_B = 0.5$ and perfect $c(2 \times 2)$ order, the 1NN shell of every atom is populated entirely by dissimilar atoms, so $p_{AB} = 1$, and $\alpha = -1$.

Figure 5 shows the MC-predicted dependence of α on temperature and strain for $x_{Pd} = 0.5$. The plots indicate that at low temperatures, the AuPd/Pd(100) surface exhibits perfect $c(2 \times 2)$ order under all three strain conditions considered. As the temperature rises, the arrangement of Au and Pd atoms in the surface becomes increasingly random; however, compressive strain is seen to significantly delay the deterioration of order.

These results clearly demonstrate that compressive strain promotes the formation of monomers and stabilizes $c(2 \times 2)$-like order in the AuPd/Pd(100) surface. To gain more insight into this finding, we turned next to examining how the surface electronic structure is modified by alloying and strain. Figure 6 shows the electron density of states (DOS) projected onto the d orbitals of Pd and Au atoms in the strain-free $c(2 \times 2)$ surface; results for the unalloyed Pd/Pd(100) and Au/Pd(100) surfaces are also shown for comparison. Formation of the $c(2 \times 2)$ surface alloy is found to significantly enhance the Pd DOS in the high binding tail about 4–6 eV below the Fermi level [Fig. 6(a), top panel]. As can be seen by comparing the top panels of Figures 6(b) and 6(c), this enhancement is due almost entirely to a downshift of in-plane $(d_{xy} + d_{x^2-y^2})$ states; the out-of-plane $(d_{xz} + d_{yz} + d_{z^2})$ states in the tail region are affected comparatively little. A concurrent upshift of Au in-plane states also occurs [Fig. 6(b), lower panel], indicating significant hybridization between the in-plane Au 5d and Pd 4d states, which may contribute to the stability of the $c(2 \times 2)$ surface.

To better understand the relative stability of different arrangements of surface atoms under different strain conditions, we compared the $c(2 \times 2)$ surface and a $p(4 \times 2)$-ordered surface which is shown schematically in Figure 7; the $p(4 \times 2)$ surface has the same composition ($x_{Pd} = 0.5$) but a smaller number of Au-Pd nearest neighbors. As expected, the $c(2 \times 2)$ surface is energetically more favorable than the $p(4 \times 2)$, and the difference is greatest under compression and least under tension. The strain effect on the relative stability of the two surfaces is clarified by the following electronic structure analysis.

As shown in Figure 8, under all three strain conditions considered, the Pd d DOS of both surfaces show enhancement in the tail region (below around −4 eV from the Fermi level); this is due apparently to in-plane Au 5d-Pd 4d hybridization. The two surfaces nonetheless differ in that the enhancement is consistently more pronounced in $c(2 \times 2)$,

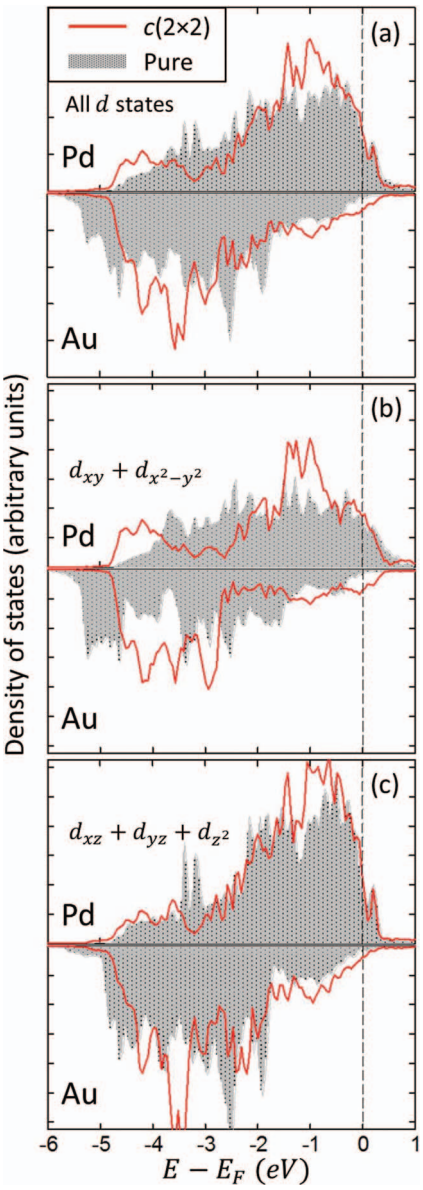

FIG. 6. Surface Pd d DOS (red line, upper panels) and Au d DOS (red line, lower panels) for the strain-free $c(2 \times 2)$ surface, compared to their respective pure surfaces, Pd/Pd(100) and Au/Pd(100) (gray backgrounds). All plots have been normalized independently and shifted to place the Fermi energy at 0 eV. For clarity, the scales of the graphs showing the in-plane $(d_{xy} + d_{x^2-y^2})$ (b) and out-of-plane $(d_{xz} + d_{yz} + d_{z^2})$ (c) components have also been magnified 2 × relative to the total (a).

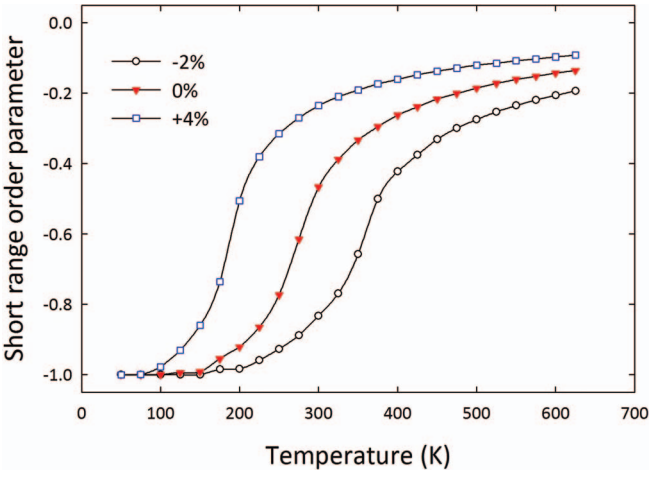

FIG. 5. Short-range order as a function of temperature and strain (−2%, 0%, and 4%) when $x_{Pd} = 0.5$.

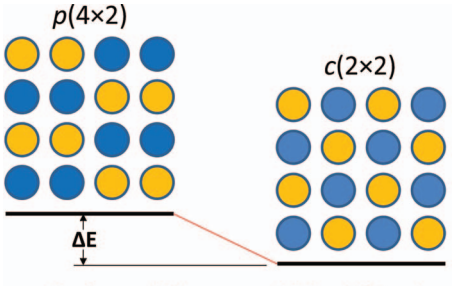

Strain condition	ΔE (meV/atom)
-2% (compression)	18.0
0% (strain-free)	14.2
+4% (tension)	10.2

FIG. 7. Strain-dependent differences in the DFT-calculated total energies of the $p(4 \times 2)$ and $c(2 \times 2)$ surfaces that we examined.

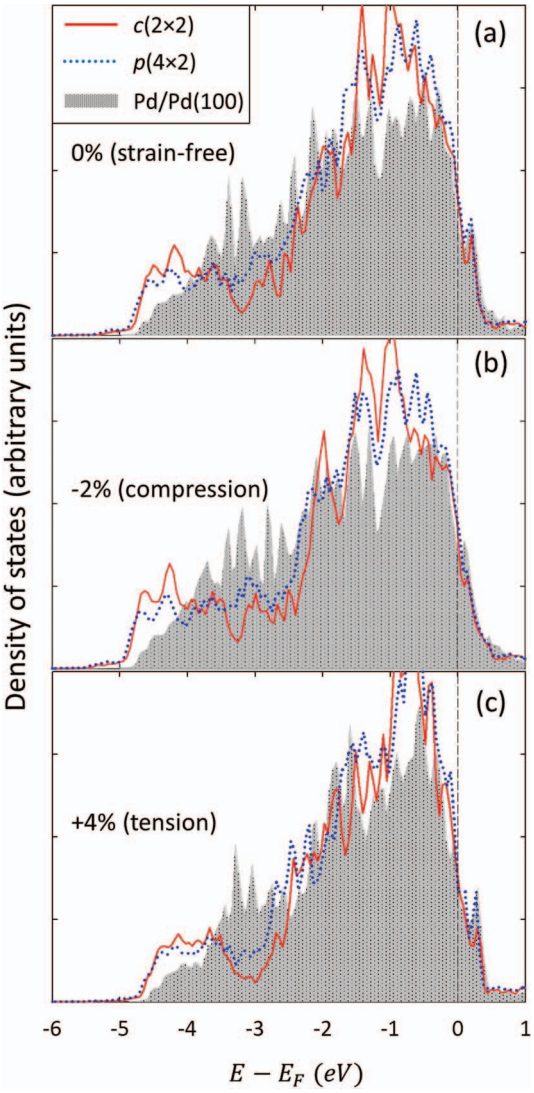

FIG. 8. Surface Pd*d* DOS for the $c(2 \times 2)$ (red, solid line) and $p(4 \times 2)$ (blue, dotted line) surfaces compared to Pd/Pd(100) (gray background) under different strain conditions. All plots have been normalized independently and shifted to place the Fermi energy at 0 eV.

due to its larger number of Au-Pd neighbors. This difference is visibly largest when the surfaces undergo compression [Fig. 8(b)] and smallest when they undergo tension [Fig. 8(c)], paralleling the trend in their relative stability as described earlier. This suggests that compressive strain stabilizes $c(2 \times 2)$-like order (and also promotes monomer formation) by, at least in part, magnifying the effects of in-plane *d-d* hybridization between neighboring Au and Pd atoms.

Although there are no experimental data currently available for direct comparison, our theoretical study clearly highlights significant impact of strain on the atomic arrangement of surface alloys, which is also likely to affect their surface chemistry. One could impose a biaxial strain of a few percent on a thin metal film through the lattice mismatch between the film and the underlying substrate. Alternately, it would be also possible to examine the strain effect by externally stressing a free-standing sample. Moreover, in core-shell nanocatalysts, lattice strain has been found to significantly influence their catalytic activity by modifying the surface properties.[45,46] Perhaps, significant strain may also cause a change in the configuration of subsurface atoms and/or induce mixing with the substrate, which could in turn influence the surface atomic ordering. However, in this work, we intend to focus on the strain effects on the interatomic interactions and consequent ordering tendencies in the AuPd surface alloy using the simple AuPd/Pd system; further studies are warranted to examine the effect of subsurface/bulk composition on surface atomic arrangement.

IV. SUMMARY

Monte Carlo (MC) simulations were performed to examine the effects of applied strain on the finite-temperature arrangement of atoms in AuPd/Pd(100) surface alloys. In this work, three strain conditions were considered (0%, 2% compression, and 4% tension); strain was measured relative to the bulk Pd lattice and applied biaxially, parallel to the surface. For each of the three strain cases, a separate cluster expansion (CE) Hamiltonian for use in the MC simulations was developed from the results of density functional theory (DFT) calculations. Pair interactions up to the fifth nearest-neighbor (5NN) distance and 3- and 4-body interactions up to the 4NN distance were considered for inclusion in the CE models. Our MC simulations show that the application of strain can result in dramatically different arrangements of surface atoms. In particular, compressive strain was seen to increase the number of Pd monomers relative to the strain-free case, and tensile strain was seen to reduce it. The number of second nearest-neighbor pairs of Pd monomers was similarly enhanced by compressive strain, as was short range, $c(2 \times 2)$-like order. We also performed an electronic structure analysis of the AuPd/Pd(100) system in order to understand the origin of these strain effects. We found that enhanced hybridization between in-plane Au and Pd *d* states under biaxial compression helps to stabilize the $c(2 \times 2)$ surface and may also explain the increased population of Pd monomers and second nearest-neighbor monomer pairs. By highlighting the influence of strain over the atomic configuration of surface alloys, our findings may suggest an additional role for strain

engineering, beyond the well-known relationship between strain and surface electronic structure, in the rational design of alloy catalysts.

ACKNOWLEDGMENTS

We acknowledge the Robert A. Welch Foundation (F-1535) and the National Science Foundation (NSF-IGERT Grant DGE-0549417) for the support of this work. All our calculations were performed using supercomputers at the Texas Advanced Computing Center at the University of Texas.

[1]J. K. Edwards, B. E. Solsona, P. Landon, A. F. Carley, A. Herzing, C. J. Kiely, and G. J. Hutchings, J. Catal. **236**, 69 (2005).
[2]J. K. Edwards, A. F. Carley, A. A. Herzing, C. J. Kiely, and G. J. Hutchings, Faraday Discuss. **138**, 225 (2008).
[3]M. Chen, D. Kumar, C.-W. Yi, and D. W. Goodman, Science **310**, 291 (2005).
[4]M. Chen, K. Luo, T. Wei, Z. Yan, D. Kumar, C. Yi, and D. W. Goodman, Catal. Today **117**, 37 (2006).
[5]D. Kumar, M. Chen, and D. W. Goodman, Catal. Today **123**, 77 (2007).
[6]D. I. Enache, J. K. Edwards, P. Landon, B. Solsona-Espriu, A. F. Carley, A. A. Herzing, M. Watanabe, C. J. Kiely, D. W. Knight, and G. J. Hutchings, Science **311**, 362 (2006).
[7]H. C. Ham, G. S. Hwang, J. Han, S. W. Nam, and T. H. Lim, J. Phys. Chem. C **113**, 12943 (2009).
[8]H. C. Ham, G. S. Hwang, J. Han, S. W. Nam, and T. H. Lim, J. Phys. Chem. C **114**, 14922 (2010).
[9]H. C. Ham, J. A. Stephens, G. S. Hwang, J. Han, S. W. Nam, and T. H. Lim, J. Phys. Chem. Lett. **3**, 566 (2012).
[10]D. Wang, A. Villa, F. Porta, L. Prati, and D. Su, J. Phys. Chem. C **112**, 8617 (2008).
[11]F. Maroun, F. Ozanam, O. M. Magnussen, and R. J. Behm, Science **293**, 1811 (2001).
[12]C.-W. Yi, K. Luo, T. Wei, and D. W. Goodman, J. Phys. Chem. B **109**, 18535 (2005).
[13]T. Wei, J. Wang, and D. W. Goodman, J. Phys. Chem. C **111**, 8781 (2007).
[14]P. Han, S. Axnanda, I. Lyubinetsky, and D. W. Goodman, J. Am. Chem. Soc. **129**, 14355 (2007).
[15]J. A. Boscoboinik, C. Plaisance, M. Neurock, and W. T. Tysoe, Phys. Rev. B **77**, 045422 (2008).
[16]J. A. Boscoboinik, F. C. Calaza, M. T. Garvey, and W. T. Tysoe, J. Phys. Chem. C **114**, 1875 (2010).
[17]M. Garvey, J. A. Boscoboinik, L. Burkholder, J. Walker, C. Plaisance, M. Neurock, and W. T. Tysoe, J. Phys. Chem. C **116**, 4692 (2012).
[18]J. A. Stephens, H. C. Ham, and G. S. Hwang, J. Phys. Chem. C **114**, 21516 (2010).
[19]J. A. Stephens and G. S. Hwang, J. Phys. Chem. C **115**, 21205 (2011).
[20]E. Kampshoff, E. Hahn, and K. Kern, Phys. Rev. Lett. **73**, 704 (1994).
[21]M. Mavrikakis, B. Hammer, and J. K. Nørskov, Phys. Rev. Lett. **81**, 2819 (1998).
[22]Y. Xu and M. Mavrikakis, Surf. Sci. **494**, 131 (2001).
[23]E.-K. Whang, J. Oh, S.-K. Kim, J.-S. Kim, and G. Lee, Phys. Rev. B **63**, 075401 (2001).
[24]A. Schlapka, M. Lischka, A. Groß, U. Käsberger, and P. Jakob, Phys. Rev. Lett. **91**, 016101 (2003).
[25]S. Murphy, G. Mariotto, N. Berdunov, and I. Shvets, Phys. Rev. B **68**, 165419 (2003).
[26]A. Roudgar and A. Groß, J. Electroanal. Chem. **548**, 121 (2003).
[27]L. Grabow, Y. Xu, and M. Mavrikakis, Phys. Chem. Chem. Phys. **8**, 3369 (2006).
[28]M. Tsuda and H. Kasai, Phys. Rev. B **73**, 155405 (2006).
[29]Y. Gohda and A. Groß, J. Electroanal. Chem. **607**, 47 (2007).
[30]J. M. Sanchez, F. Ducastelle, and D. Gratias, Physica A **128**, 334 (1984).
[31]J. W. D. Connolly and A. R. Williams, Phys. Rev. B **27**, 5169 (1983).
[32]L. G. Ferreira, S. Wei, and A. Zunger, Phys. Rev. B **40**, 3197 (1989).
[33]D. B. Laks, L. G. Ferreira, S. Froyen, and A. Zunger, Phys. Rev. B **46**, 12587 (1992).
[34]V. Blum and A. Zunger, Phys. Rev. B **69**, 020103 (2004).
[35]V. Blum and A. Zunger, Phys. Rev. B **70**, 155108 (2004).
[36]S. V. Barabash, V. Blum, A. Zunger, and S. Müller, Phys. Rev. B **74**, 035108 (2006).
[37]K. Yuge, A. Seko, F. Oba, A. Kuwabara, and I. Tanaka, Phys. Rev. B **76**, 045407 (2007).
[38]A. van De Walle and G. Ceder, J. Phase Equilib. **23**, 348 (2002).
[39]See supplementary material at http://dx.doi.org/10.1063/1.4825396 for the cluster expansions used in this study along with some additional details pertaining to their creation.
[40]J. Perdew and Y. Wang, Phys. Rev. B **45**, 13244 (1992).
[41]G. Kresse and J. Furthmüller, *VASP the Guide* (Vienna University of Technology, Vienna, Austria, 2001).
[42]P. E. Blöchl, Phys. Rev. B **50**, 17953 (1994).
[43]C. Kittel, *Introduction to Solid State Physics* (John Wiley and Sons, 2005).
[44]J. Cowley, Phys. Rev. **77**, 669 (1950).
[45]J. X. Wang, H. Inada, L. J. Wu, Y. M. Zhu, Y. M. Choi, P. Liu, W. P. Zhou, and R. R. Adzic, J. Am. Chem. Soc. **131**, 17298 (2009).
[46]P. Strasser, S. Koh, T. Anniyev, J. Greeley, K. More, C. F. Yu, Z. C. Liu, S. Kaya, D. Nordlund, H. Ogasawara, M. F. Toney, and A. Nilsson, Nat. Chem. **2**, 454 (2010).